COMPDYN 2011
3rd ECCOMAS Thematic Conference on
Computational Methods in Structural Dynamics and Earthquake Engineering
M. Papadrakakis, M. Fragiadakis, V. Plevris (eds.)
Corfu, Greece, 25–28 May 2011

SEISMIC RETROFIT OF EXISTING STEEL MOMENT RESISTING FRAMES WITH INNOVATIVE MATERIALS: LARGE SCALE HYBRID SIMULATION TESTS

Dimitrios G. Lignos[1], **Daniel M. Moreno-Luna**[2], **and Sarah L. Billington**[2]

[1] McGill University
817 Sherbrooke West, Room 278C, Montreal, QC, H3A 2K6
e-mail: dimitrios.lignos@mcgill.ca

[2] Stanford University
John A. Blume Earthquake Engineering Center, 439 Panama at Duena, Building 540, Stanford, CA, 94305
email 1: danielm3@stanford.edu, email 2: billington@stanford.edu

Keywords: Seismic Retrofit, Steel Moment Frames, Hybrid Testing, High Performance Fiber Reinforced Cementitious Materials.

Abstract. *This paper discusses the experimental validation of a new system for seismic retrofit of existing steel moment resisting structures. The system consists of infill panels made of a High Performance Fiber Reinforced Concrete (HPFRC) that is able to strain harden in tension. A two-phase experimental program was designed and conducted at the Network for Earthquake Engineering Simulation (NEES) facility at the University of California, Berkeley. This program utilized large-scale hybrid simulations of a 2/3-scale, 2-story steel moment frame designed in 1980s retrofitted with HPRFC infill panels. The numerical challenges during the experimental program including the development of a phenomenological model that is able to simulate cyclic deterioration of the HPFRC infill panels are summarized and validated with the available experimental data.*

1 INTRODUCTION

The goal of seismic rehabilitation strategies is to effectively upgrade seismically deficient structures that do not meet a designated performance objective. The performance objective could be achieving a specified performance level such as Immediate Occupancy (IO), Life Safety (LS) or Collapse Prevention (CP). Guidelines for seismic evaluation and rehabilitation are summarized in ATC 40 [1], FEMA 356 [2] and FEMA 440 [3].

A common way to improve the seismic performance of an existing steel moment resisting frame (MRF) involves the modification of the structural system to enhance its global strength and/or stiffness in order to avoid excessive story drift ratios during an earthquake (see FEMA 351 [4] and FEMA 547 [5]). Because MRFs are more flexible compared to other types of lateral resisting systems such as steel braced frames, an additional concern is the concentration of plastic deformations at the bottom stories due to P-Delta effects. Another common seismic deficiency in steel MRFs is brittle beam-to-column connections that are not able to develop sufficient plastic deformation capacity during an earthquake. Such types of component failures were notable during the Northridge 1994 earthquake in California (see FEMA 351 [4]) and also the Kobe 1995 earthquake in Japan. Pre-Northridge welded moment resisting connections typically consist of bolted shear tabs with full penetration welded flanges. Typical rehabilitation techniques summarized in [5] are concerned with the addition of a steel braced frame, concrete or masonry shear wall to the existing steel MRF to control excessive story deformations. Another way to improve the seismic performance of an existing steel MRF is to enhance the beam-to-column moment connections to develop a minimum plastic deformation of 2% radians. Typically, the bolted bracket (Adan and Gibb [6]) welded hunch (Gross et al. [7], Civjan et al. [8]) and RBS approach (Uang et al. [9]) are three standard connection rehabilitation techniques that are used.

Recently, High Performance Fiber Reinforced Concrete (HPFRC) materials have been utilized for seismic retrofit applications including reinforced concrete (RC) and coupled wall systems (Hung and El-Tawil [10, 11]), and steel moment resisting frames (Kesner and Billington [12]). The advantage of these composites is that they are characterized by pseudo-ductile tensile strain hardening behavior and energy absorption prior to crack localization and they exhibit little to no spalling in compression.

This paper discusses the development and experimental validation of the seismic retrofit system originally developed by [12]. A two-phase testing program was designed and executed that utilized large-scale hybrid simulations of an existing 2-story steel MRF designed in 1980s and retrofitted with the HPFRC infill panel system. These tests were conducted at the large-scale facility at the Richmond Field Station of the University of California at Berkeley, which is part of the Network for Earthquake Engineering Simulation (NEES). The hybrid simulation tests together with the experimental program that was conducted on single and double HPFRC infill panel components offered the opportunity to develop and validate 2-dimensional numerical models of retrofitted existing steel MRF with HPFRC infill panels.

2 HIGH PERFORMANCE FIBER REINFORCED CONCRETE

A modified version of the self-compacting high performance fiber-reinforced concrete mix that was developed by Liao et al. [13] at University of Michigan is used in this research. This mix has self-compacting properties and very minimal vibration is used to aid in consolidation. The mix proportion that is used has a water-to-binder ratio of 0.40 with the binder consisting of 80% type I-II Portland cement and 20% Class C fly ash. The super plasticizer used is ADVA Cast 530 and is added at 0.4% of the binder weight. A viscous agent is also used and is added at 0.49% of the binder weight. The fine aggregate is regular sand of uniform size distribution that can be easily found in any commercial precasting plant in California. A 12.7mm maximum coarse aggregate is also used, which is locally available. High strength hooked steel fibers marked as Dramix RC-80/30-BP are used in the HPFRC mix at 1.2% of the mix by volume. The minimum specified tensile strength of the fibers is 2300MPa. A regular concrete mixer that can be found in a precast plant can be utilized to mix the HPFRC material. In addition, Olsen and Billington [14, 15] and Hanson and Billington [16] have also used typical drum mixers to mix the same material. The mixing sequence is described in detail in [14, 16]. For the concrete mixes 102mmx203mm cylinders are cast and tested in compression to obtain the compression strength of the mix. A typical compression stress versus strain deformation curve for the HPRFC mix is shown in Figure 1a. To obtain the tensile properties of the same mix 76mmx76mmx305mm beams are cast and tested using 3-point bending following ASTM standard C 1609/C (ASTM [17]). The equivalent stress versus strain of a set of 4 of those beams is shown in Figure 1b. The equivalent stress is computed based on the following relationship,

$$\sigma_{b,equiv.} = \frac{Pl}{bd^2} \tag{1}$$

in which, P is the actuator load, l is the clear span length, d and b are the depth and width of the beam, respectively. As seen from the same figure the mix can carry flexural tension with a ductility range from 3 to about 6. Here, ductility is defined as the ratio between ultimate deformation prior to strength deterioration and the yield deformation of the HPRFC beam.

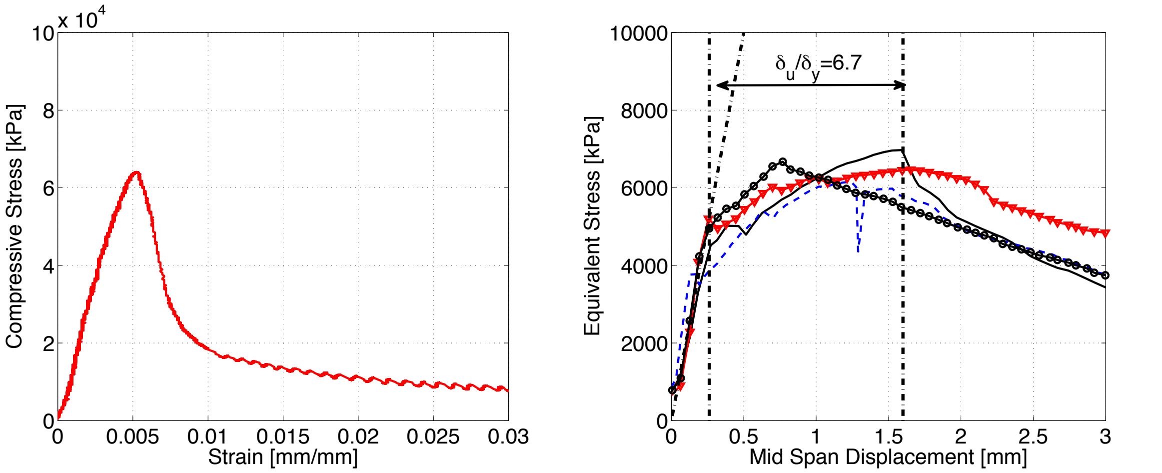

(a) Compressive strength versus strain (b) Equivalent stress versus mid span displacement

Figure 1: Mechanical properties of High Performance Fiber Reinforced Concrete.

3 PROPOSED RETROFIT SYSTEM FOR SEISMIC REHABILITATION

The design mix discussed in Section 2 is used for the fabrication of the proposed HPFRC infill panel system for seismic retrofit of steel MRFs. This system is shown in Figure 2a. The HPFRC infill panels utilize Welded Wire Fabric (WWF) to aid in shear reinforcement and bolster flexural strength. The WWF is a single layer of 10 gauge wire on a 76mmx76mm grid. Grade 50 #3 deformed mild steel consists the primary reinforcement. Each set of two vertical HPFRC infill panels are first grouted into each of two steel channel connections that are shown in Figures 2a and 2b. These connections are pre-tensioned to about 150kN in order to avoid any slip in the connection. For this purpose a load-indicating washer is used. The top steel channel connection is field welded at the bottom flange of the upper floor steel beam.

The bottom channel connection is bolted to threaded studs that are welded to the top flange of the steel beam of the bottom story. The procedure to be used to weld these studs on the top flange of the bottom steel beam is a proven construction technique referred to by Nelson Stud Welding Inc. Holes are cored into the existing slab of a building exposing the top flange of the steel beam, and new headed studs are welded through the cored hole and then grouted in place to achieve composite construction where non-composite action was originally designed.

The two HPFRC panels are connected at mid-height of a story with a slotted connection shown in Figure 2a. This connection is utilized in order to prevent any build up of axial load in the HPFRC panels and subsequently any out-of-plane movement of the double panel system. The middle connection also guarantees that the inflection point of the bending diagram of the HPFRC double panel system stays at mid-height during the entire response history of the retrofitted steel MRF. The bolted connection details allow for damaged panels to be removed and replaced quickly after a major earthquake event provided that the residual story deformations are not large after that major earthquake event.

For panel fabrication, the infill panels are cast into plywood molds (see Figure 2c). The exposed surface of the HPFRC infill panel is finished relatively smooth without much difficulty. A number of single and double infill panels have been tested at University of Michigan in order to investigate their hysteretic response [14, 15, 16]. An example can be seen in Figure 2d. In the same figure, we have superimposed the simulated response of these panels with a phenomenological model that can capture pinching and cyclic deterioration and is utilized later to investigate numerically the seismic performance of the retrofitted steel MRF.

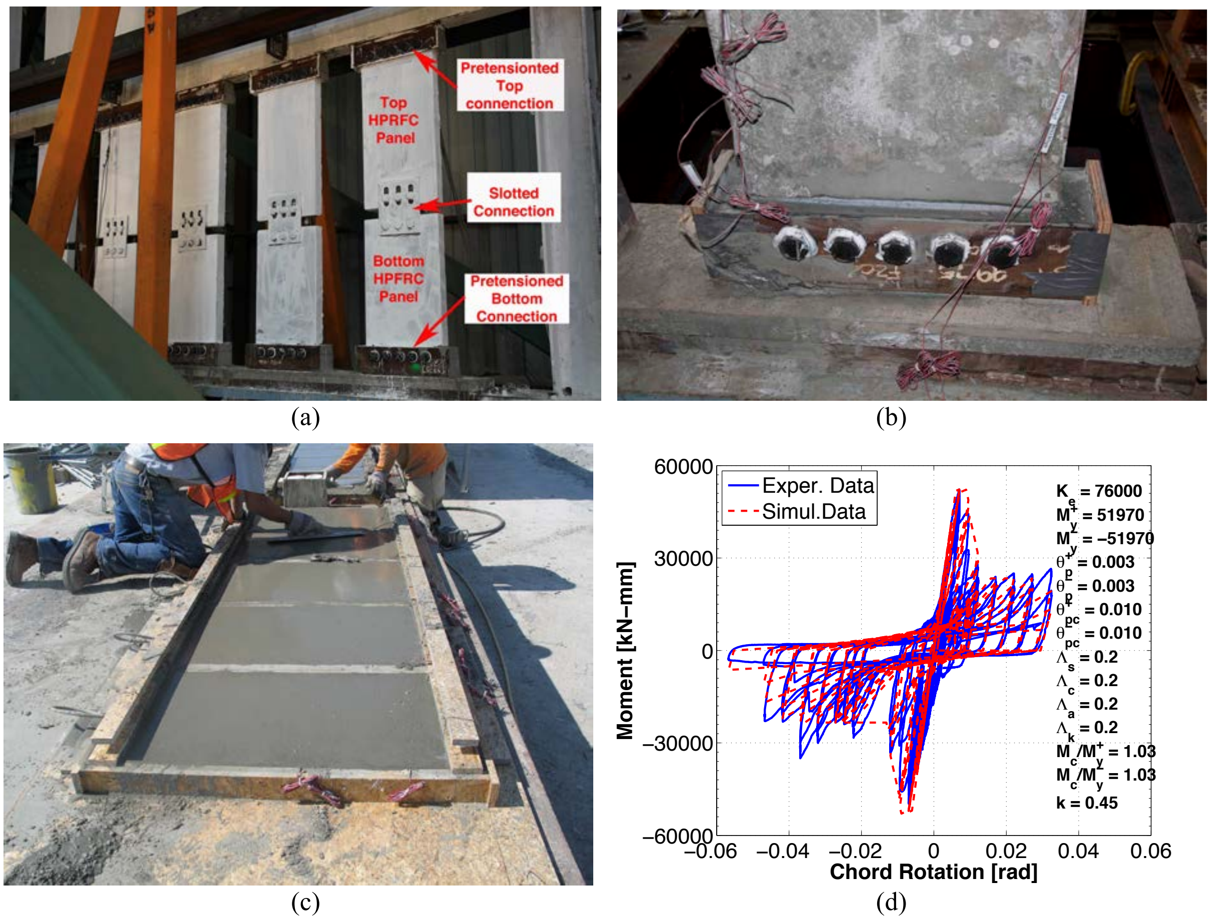

Figure 2: Installation, fabrication and hystereric performance of the HPFRC infill panel system for seismic retrofit applications.

4 PROTOTYPE STEEL STRUCTURE

In order to evaluate the performance of the infill panel system as part of a structural system, a prototype steel structure that was designed in California in 1980s is used. This structure, which is shown in Figure 3a in plan view, consists of perimeter steel moment resisting frames. The geometry of the East West (EW) steel MRF of the steel structure is shown in elevation in Figure 3b. The predominant period of this structure is 0.75sec. This structure does not meet the retrofit objectives per ASCE 41 [18] and FEMA 356 [2]. The EW steel MRF is modeled in the OpenSees [19] simulation platform using elastic beam column elements with nonlinear rotational springs at their ends. These springs can simulate component deterioration based on the modified Ibarra-Krawinkler (IK) model (Ibarra et al. [20], Lignos and Krawinkler [21, 22]). Panel zones are modeled with the Krawinkler model [23] as discussed in Gupta and Krawinkler [24]. The modified IK model is able to simulate fracture of steel connections based on a Coffin-Mansion fracture rule that was implemented by Lignos et al. [24]. Information related to premature steel beam-to-column connection fractures is obtained from a recently developed steel database for deterioration modeling of steel beams [21, 22].

In order to retrofit the 2-story building shown in Figure 3, a set of five panels is installed in the exterior left bay of the EW steel MRF of the prototype structure. Since there are no established design guidelines for this type of retrofit, the HPRFC infill panel system is assumed to be a deteriorating element. This assumption is valid since this retrofit system dissipates energy through multi-cracking of the HPRFC infill panels. After a few number of cycles the infill panels deteriorate as shown in Figure 2d.

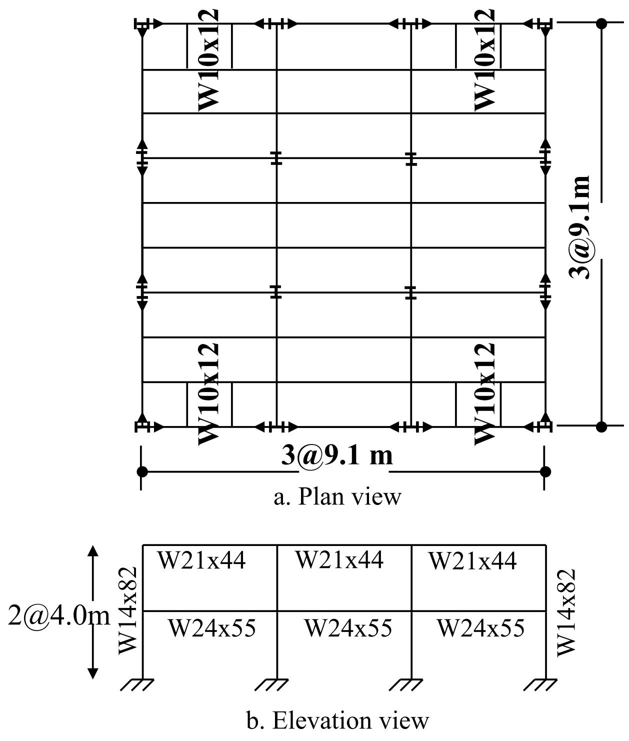

Figure 3: Plan view and elevation of the prototype steel office building designed in 1980s in California.

5 LARGE SCALE HYBRID SIMULATIONS

In order to validate experimentally the seismic performance of the retrofitted EW steel MRF discussed in Section 4, a 2/3-scale model of this moment frame is designed and fabricated. Strength and stiffness of this frame are scaled based on similitude rules discussed in

Moncarz and Krawinkler [25] and Harris and Sabnis [26]. The web and flange slenderness ratios of these sections were carefully selected in order to match the target deterioration parameters of the steel components of the prototype building shown in Figure 3b. State-of-the-art hybrid simulations are utilized in order to test experimentally the retrofitted steel MRF. The subsequent sections present aspects of hybrid testing including the hybrid model, experimental setup, and instrumentation.

5.1 Hybrid Model

Hybrid simulation is utilized in order to evaluate the seismic performance of the retrofitted steel MRF with HPFRC infill panels. Hybrid simulation is an experimentally based method for investigating the response of a structure to dynamic excitation using a hybrid model that consists of a physical and a numerical subassembly [27, 28]. The physical subassembly is tested in the laboratory. In this case, the physical subassembly is the first bay of the retrofitted steel MRF with the HPFRC panels installed. Typical A992 Gr. 50 steel is used for fabrication of the steel beams and columns of the 2/3-scale steel MRF shown in Figure 4a. Based on tensile coupon tests the yield and ultimate strengths of these components are summarized in Table 1. In order to simulate as realistically as possible the HPFRC pre-tensioned connection boundary conditions a 60mm concrete slab is cast at the base and second and third floor beams as shown in Figure 4b. In order to secure fixed conditions at the base a 51mm steel plate is used and the steel columns are welded with a typical CJP weld as shown in Figure 4c. The bolted web-welded flange beam-to-column connections of the test subassembly are welded in the field with a typical CJP weld. Figure 4d shows an example of these connections.

(a) steel MRF installed on the self-reacting platform

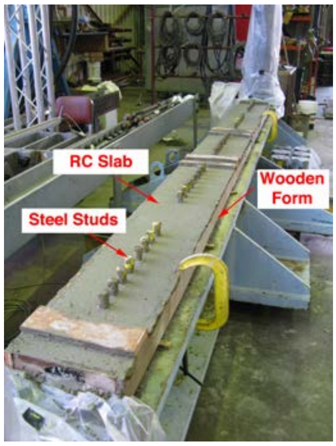

(b) ground floor RC slab after casting

(c) fixed column base

(d) beam-to-column connection and slider

Figure 4: Erection and typical connection details of the physical subassembly part of the hybrid model.

Wide Flange Section	Measured Material Properties		
	Location	σ_y (N/mm^2)	σ_u (N/mm^2)
W10x30	Flange	358	448
	Web	381	465
W14x26	Flange	363	449
	Web	385	467
W10x45	Flange	366	440
	Web	384	466

Table 1: Material properties of W sections of the physical subassembly tested in the laboratory.

The numerical portion of the hybrid model is modeled in the OpenSees [19] analysis platform in the same way that was previously discussed in Section 4. A schematic representation of the hybrid simulation technique is shown in Figure 5. As diagrammed in this figure, from a known state at instance *i* we use a numerical technique to compute a target displacement at instance *i+1*, then we use the two actuators assigned to the two horizontal degrees of freedom to impose the target displacements and measure forces and then compute the new state at instance *i+1*. The Open-source Framework for Experimental Setup and Control (OpenFresco) [29, 30] is utilized in order to conduct the hybrid simulations. As seen in Figure 5, the implementation strategy that is used separates the integrator and sub-structure processes. A three-loop architecture starts issuing actuator commands using a local estimator (predictor) of the new (target) state and then corrects the trajectory when the true target state arrives from the integrator. It should be noted that in this process the error accumulates. More details about an advanced implementation of hybrid simulation can be found in [30].

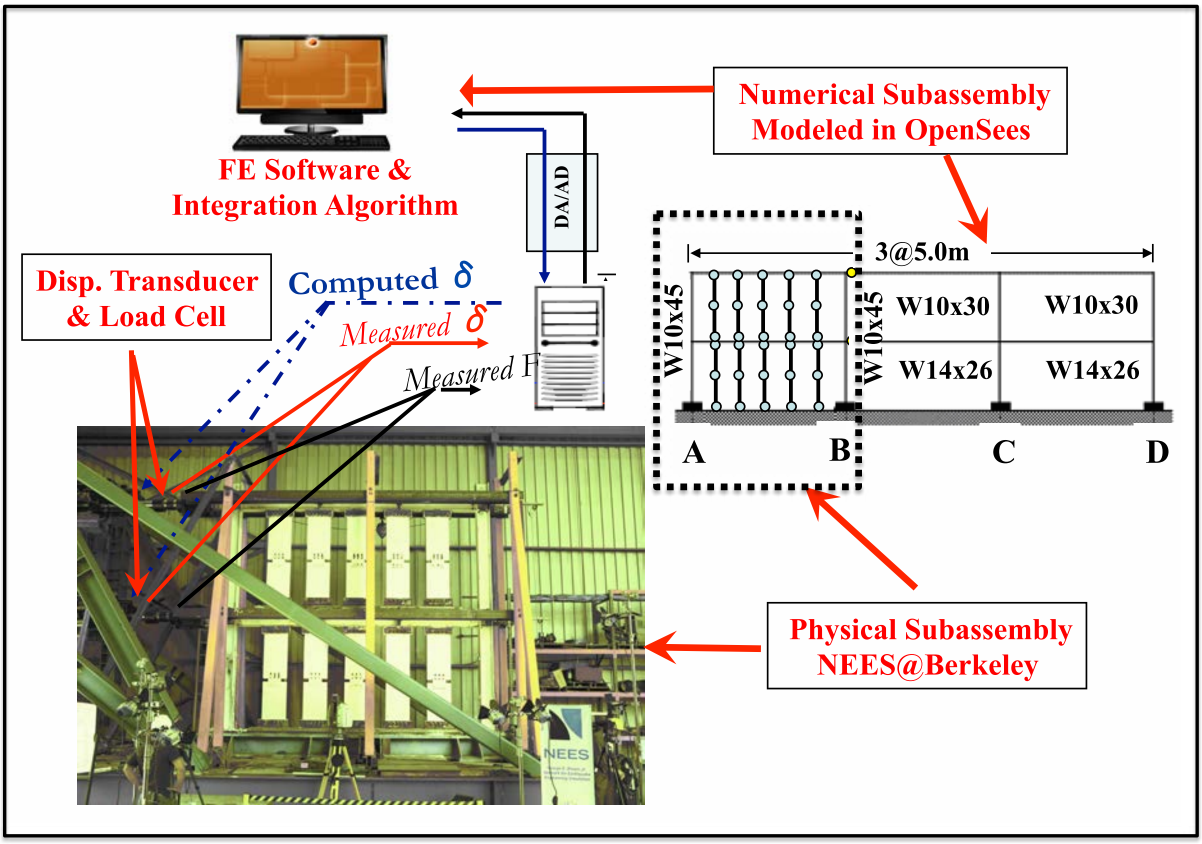

Figure 5: Schematic representation of hybrid simulation

5.2 Coupled Simulation

Prior to conducting the hybrid simulations with the physical subassembly in the laboratory, a coupled simulation was conducted with OpenFresco. The numerical subassembly of the 2-story steel MRF shown in Figure 6 is connected with a generic Super-Element within OpenSees that represents the physical subassembly tested in the laboratory. In this discussion, this is noted as the "Master Program". The physical subassembly is also modeled in OpenSees with a separate input file that herein is called the Slave Program. The HPFRC infill panels are modeled with rigid links connecting deteriorating springs that can simulate the hysteretic response and flexibility of the HPFRC panels as shown in Figure 2d. The Master Program is responsible for imposing boundary conditions on both subassemblies. The 2-node adapter element shown in Figure 6 imposes trial displacements on the "physical subassembly". The main information extracted from the coupled simulation is an estimate of the initial 2x2 stiffness matrix of the "physical subassembly" by holding one-degree-of-freedom at a time and applying a unit displacement to the other one. This matrix is,

$$K = \begin{bmatrix} 58.1 & -27.4 \\ -27.4 & 15.3 \end{bmatrix} \text{kN/mm} \tag{2}$$

Additional information that is extracted from the coupled simulation results is the integration method that is used during the hybrid simulation. A Newmark beta hybrid simulation implicit integrator is used with a constant number of sub-stepping [30]. Details about the assessment of coupled simulation results are given in Lignos and Billington [31].

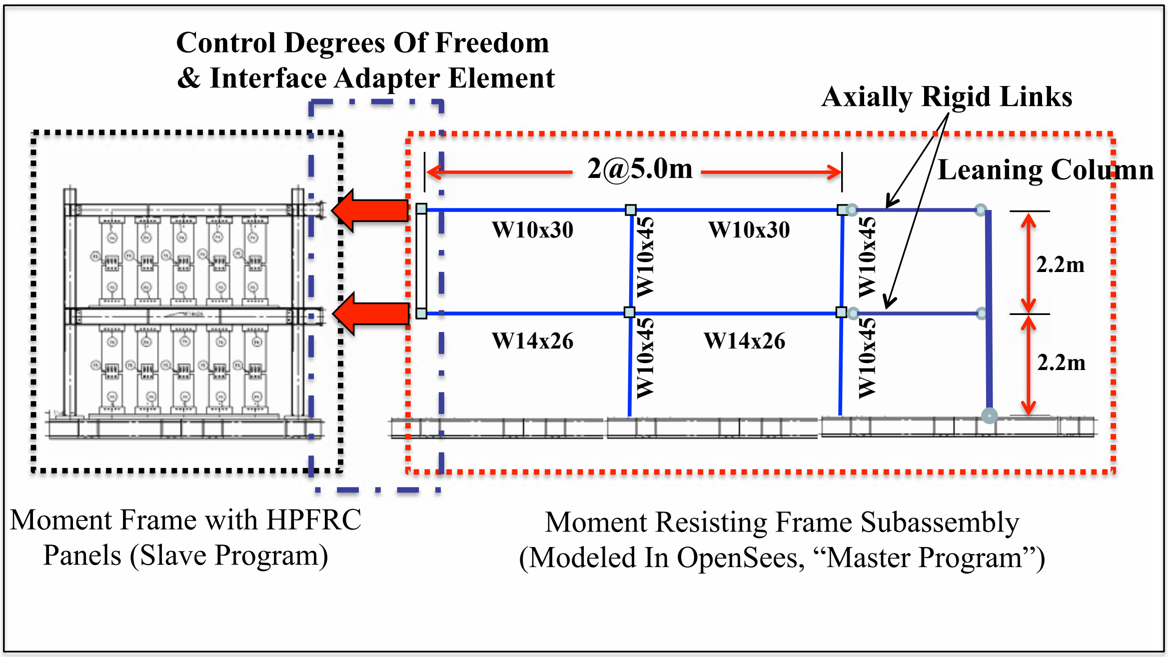

Figure 6: Schematic representation of hybrid simulation

5.3 Experimental Setup

The experimental setup of the physical subassembly tested in the Richmond Field Station at the University of California at Berkeley consists of three main parts, which are a self-reacting platform (see Figure 4a), the test frame and the lateral support system. The latter prevents any out-of-plane deformations of the test frame during the unidirectional earthquake simulation. All parts of the test setup are shown in Figure 7. Two 980kN (220-kips) dynamic actuators are connected with the test frame per floor as shown in the same figure. The self-reacting frame shown in Figure 4a was analyzed and fabricated in such a way that vertical deformations are minimized during the hybrid simulation tests. Vertical deformations of the self-reacting platform are measured with vertical LVDTs in order to make sure that they stay minimal. This platform consists of W21x166 steel sections connected together with full penetration weld. The platform is able to safely resist up to 1500kN base shear. The test frame is welded on the self-reacting platform with a 6.35mm continuous weld around the W14x311 supporting beam to guarantee full composite action between the middle interior W21x166 and W14x311 steel sections. The lateral support system consists of six triangular frames made of HSS6x6x3/8 (three on each side) and connected to each other with a longitudinal W12x26 steel beam. Lateral resistance of the lateral support frame is provided through two diagonal steel angles L6x3x1/2 that are connected at the base of the self-reacting platform. The test frame slides against this beam. The gap between the slider and the longitudinal steel beams was designed to be 6.35mm (¼”). In order to eliminate friction due to possible contact between the test frame sliders shown in Figure 4d and the W12x26 longitudinal steel beam teflon is installed in between these components. Friction forces during the hybrid simulation tests are measured through the diagonal angles that are strain gaged and calibrated to measure the force transferred to the platform due to sliding. However, during the two testing phases almost zero friction force was measured.

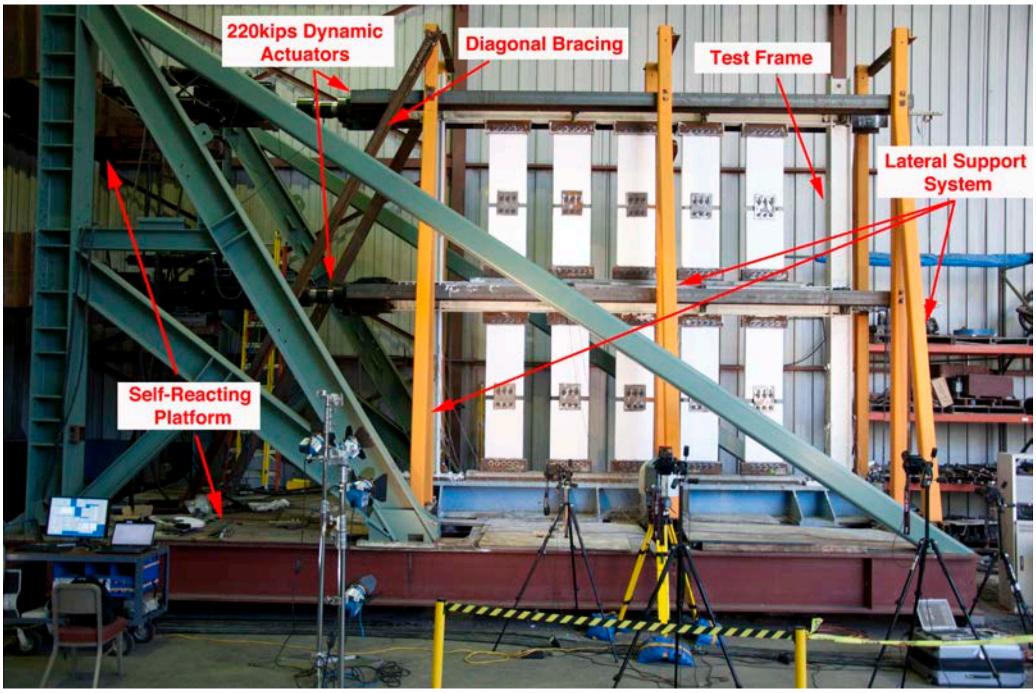

Figure 7: Experimental setup for hybrid simulation of the 2/3 retrofitted steel MRF.

5.4 Instrumentation

A total of 150 and 90 instruments are used to instrument the test frame for testing Phase I and Phase II, respectively. A laser scanner is also used that perform scan measurements of pre-defined infill panels that are likely to be damaged based on pre-test analysis predictions. The majority of instruments are strain gages to obtain strain measurements of the steel reinforcement and to obtain moment gradients in the steel columns of the test frame. One LVDT per floor is used to obtain the absolute floor displacements with respect to the “ground floor”.

Thirty-six LVDTs are attached to diagonal plastic strips to measure shear deformations in every other set of double panels per floor. A typical arrangement of these LVDTs is shown in Figure 8. Two Data Acquisition (DAQ) systems are synchronized together for the instrumentation needs of this testing series. The experimental data from both testing phases are available through the NEES central repository (www.nees.org).

Figure 8: Typical instrumentation layout of HPFRC infill panel system.

6 EXPERIMENTAL PROGRAM

Two testing phases are designed for the retrofitted steel MRF discussed in Sections 4 and 5. After the completion of testing Phase I all the HPFRC infill panels are replaced with a new set with nominally identical material properties to the ones used in testing Phase I. However, due to material variability some minor differences are noticed in the measured compressive strengths of the HPFRC panels after 28 days (see [32]). This section discusses the testing protocol used and the seismic response of the retrofitted steel MRF during the two testing phases.

6.1 Testing Protocol

Two testing phases are designed in order to conduct the large scale hybrid simulation tests of the retrofitted 2-story steel MRF. In both phases, the ground motion records are scaled appropriately to represent levels of intensity that are of particular interest to the engineering profession. Two ground motions are used for these phases. The first one is the fault normal component of the Petrolia record from the Cape Mendocino earthquake in California in 1992. The unscaled record represents a Maximum Considered Earthquake (MCE) in California with 2% probability of exceedence in 50 years at the period of interest. The second earthquake used, is the fault normal component of the Canoga Park record from the Northridge 1994 earthquake. The unscaled record of this motion represents a Design Level Earthquake (DLE) in California with 10% probability of exceedence in 50 years. The unscaled absolute acceleration and relative velocity spectra of these two motions are shown in Figures 9a and 9b, respectively. For reference, we have superimposed the predominant period of the bare steel MRF.

Testing Phase I, consists of (1) a Service Level Earthquake (SLE) with intensity equal to the 30% of the unscaled Petrolia record. This event corresponds to a 50% probability of exceedence in 50 years; (2) a DLE equal to the 70% of the unscaled Petrolia record and (3) a second DLE equal to the unscaled Canoga Park record. This event is used in order to investigate the effect of a major aftershock on the retrofitted steel MRF without replacing the

HPFRC infill panels that is likely to occur as has been illustrated during the latest earthquakes in New Zealand and Japan in 2011. Similarly, testing Phase II consists of the same SLE with testing Phase I. This part is repeated for comparison purposes. The testing protocol for this phase also consists an MCE with intensity equal to the unscaled Petrolia record in order to evaluate the seismic performance of the retrofitted steel MRF to an extreme earthquake event.

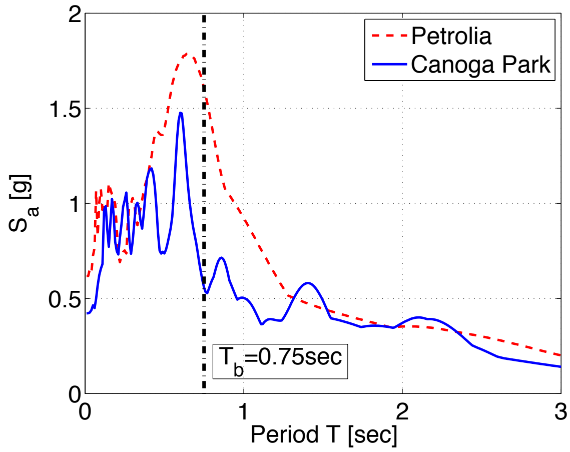

(a) Absolute acceleration spectrum

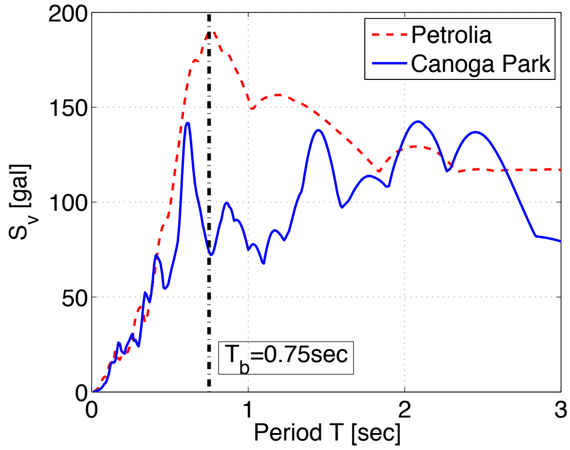

(b) Relative velocity spectrum

Figure 9: Acceleration and velocity spectra of the two ground motions used in testing Programs I and II.

7 RESULTS AND DISCUSSION

7.1 Seismic Response of the Test Frame During the Testing Program

Prior to the main testing phases the initial 2x2 stiffness of the physical subassembly was obtained by applying about one third of the yield story force per degree-of-freedom (DOF) and measuring back the relative displacements. Using the flexibility method (McGuire et al. [33]) the initial stiffness matrix is determined after coupling of the two DOF of the test frame. This matrix, which represents the Jacobian is,

$$K = \begin{bmatrix} 60.4 & -24.4 \\ -25.4 & 19.4 \end{bmatrix} \text{kN/mm} \tag{3}$$

After comparing this matrix with the one from (2) the estimated initial stiffness K based on coupled simulation is fairly close with the experimentally obtained one.

Figure 10 shows the roof drift ratio of the retrofitted steel MRF during testing Phases I and II. As seen from these figures, for both SLE phases the retrofitted test frame did not exceed more than 1% roof drift ratio. During the SLE loading, micro-cracking occurred in the HPFRC infill panels. The effect of micro cracking of HPFRC panels on the hysteretic response of the retrofitted frame can be seen in Figure 11a. This figure shows a comparison of the normalized base shear V/W versus first story drift ratio (SDR_1) during SLE for testing Phases I and II. During DLE-I (70% Petrolia) the retrofitted test frame reached slightly more than 2% rad in absolute maximum roof drift ratio and a minor residual roof drift ratio equal to 0.4% radians. Few flexural cracks were observed in the HPFRC panels. Three HPFRC infill panels failed completely at their base connection due to bending and after this failure the HPFRC panels were rocking. This implies that after DLE-I minimal to no replacement of HPFRC infill panels is needed. Without replacing any panels, the retrofitted steel MRF is subjected to a new design level earthquake (DLE-II). During DLE-II, the test frame reached a 2.5% absolute maximum roof drift ratio as shown in Figure 10a and a residual roof drift ratio of about 0.5% radians in the opposite direction compared to DLE-I. More distributed cracking was observed to the edge infill panels compared to the ones that were closer to the center of the steel beams. When reaching about 2.5% story drift ratios most of the HPFRC panels were severally damaged as discussed in [32]. These results are comparable with earlier findings of the hysteretic response of the HPFRC single and double component tests discussed in [14, 15, 16]. A comparison of peak story drift ratios between and the retrofitted steel MRF and the bare steel MRF during DLE-II is shown in figure 11b.

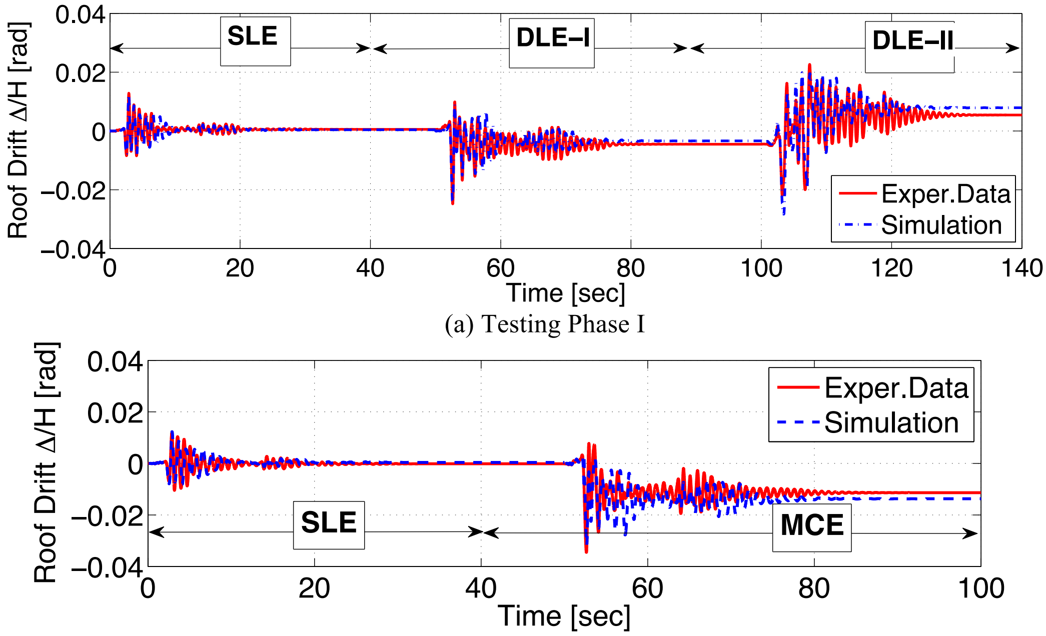

(a) Testing Phase I

(b) Testing Phase II

Figure 10: Roof drift histories of retrofitted steel MRF during testing Phases I and II.

After the completion of testing Phase I all the HPFRC infill panels were replaced by a new set with nominally identical material properties. However, due to material variability the compressive and tensile strength of the new set was slightly lower compared to the first set of infill panels [32]. During testing Phase II, a Maximum Considered Earthquake followed the

SLE in order to investigate the performance of the retrofitted steel MRF when subjected to an extreme earthquake event. Figure 10b shows the roof drift ratio of the test frame for the MCE. In the same figure we have superimposed the simulated roof drift history of the numerical model used to simulate the seismic response of the retrofitted steel MRF during both testing phases. As seen from Figure 10 the numerical simulation results match relatively well the measured experimental data.

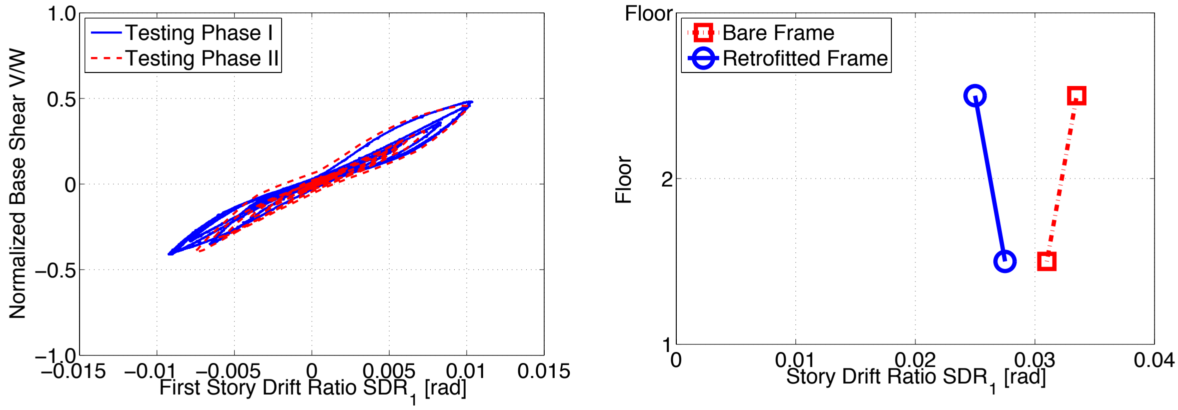

(a) (b)

Figure 11: Seismic performance of retrofitted steel MRF during testing Phase I; (a) normalized base shear versus first story drift ratio; (b) comparison of peak story drift ratios between retrofitted and bare steel MRF.

Due to large inelastic cycles prior to the main pulse of the Petrolia record (MCE) more distributed flexural cracks were developed in the HPFRC infill panels compared to Phase I. A typical damage pattern of the HPFRC infill panels after the MCE event is shown in Figure 12a. The final failure mode of a panel is the same with the one observed in Figure 12b. In some panels spalling of the reinforcement cover was observed (see Figure 12b). After the MCE event all the panels were severally damaged. The damage pattern in the HPFRC infill panels was consistent for both testing Phases I and II.

(a) multi-cracking (b) flexural crack and spalling

Figure 12: Damage pattern of HPFRC infill panels after the MCE during testing Phase II.

7.2 Structural Damage Observations and Comparison with Bare Frame Response

During testing Phase I, the structural damage that was observed to the retrofitted steel MRF was light. Yielding occurred at both the first and second floor steel beams of the steel MRF. Figures 13a and 13b shows a typical damage pattern of the first floor steel beam and column base, respectively, after the completion of testing Phase I. From Figure 13a there is no indication of local buckling in the steel beam. The hysteretic response of the corresponding numerical portion of the hybrid model indicated the same observation as shown in Figure 14a that shows the moment rotation relationship of one of the first floor steel beams that were part of the numerical portion of the hybrid model.

Looking at the normalized based shear versus first story drift ratio during testing Phase I (see Figure 14a), it can be seen that there is no indication of cyclic deterioration. The observed relatively small stiffness deterioration is attributed to the loss of stiffness from the severe damage of the HPFRC panels after DLE-II.

(a) first floor beam (b) column base

Figure 13: Structural damage observations during testing Phase I.

During testing Phase II, the structural damage that was observed to the steel MRF was very similar to that observed in testing Phase I. Again, no indication of local buckling was notable in any of the steel beam-to-column connections of the retrofitted steel frame. The lack of local buckling is confirmed from Figure 14c that shows the normalized base shear versus first story drift ratio for both the SLE and MCE loadings during testing Phase II. From this figure, there is no indication of cyclic strength deterioration. The unloading stiffness deterioration that is shown in this figure is attributed to the stiffness loss from the failure of HRFRC panels. An interesting observation during this testing phase is a dissipated energy mechanism because of yielding of the bottom flanges of the portions of the first and second floor steel beams between the steel channels. This yielding is attributed due to bending that was caused from the shear force that the individual panels carried during the MCE event (about 50kN). This yielding mechanism acted beneficially to the overall seismic behavior of the steel MRF since damage was distributed away from its the steel beam-to-column connections of the test frame. This yield mechanism is illustrated in Figure 14b.

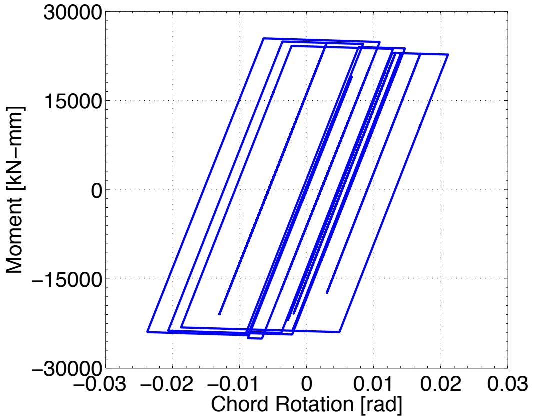

(a) Simulated moment rotation relationship of first floor steel beam during testing Phase I

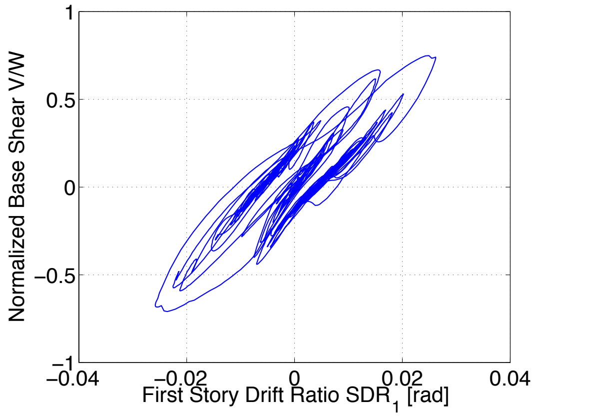

(b) Normalized base shear versus first story drift ratio of the retrofitted steel MRF during testing Phase I

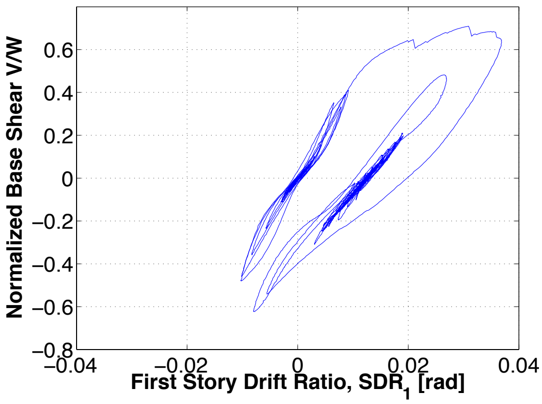

(c) Normalized base shear versus first story drift ratio of the retrofitted steel MRF during testing Phase II

(d) Observed yielding mechanism at the bottom flange of the steel beams during testing Phase II

Figure 14: Hysteretic response and observed dissipated energy mechanism during testing Phases I and II.

8 CONCLUSIONS

This paper discusses the development of an innovative seismic retrofit system for existing steel moment resisting frames designed in accordance with old seismic provisions. This system utilizes High Performance Fiber Reinforced Concrete and through multi-cracking dissipates energy during an earthquake. The proposed retrofit system was validated both numerically and experimentally through large-scale hybrid simulation tests at the NEES facility at University of California at Berkeley. Two testing phases were designed and conducted that included earthquake events of particular interest to the engineering profession. In this paper, the major computational challenges for numerical modeling of the steel moment frame and execution of the large-scale hybrid simulations were also summarized. The main findings from this research program are summarized as follows:

- Through micro cracking, the proposed infill panel system dissipates energy during service level earthquakes.
- During a Design Level or a Maximum Considered Earthquake the HPFRC infill panel system reduces seismic demands in terms of story and residual drift ratios compared to the un-retrofitted bare frame.

- Without replacing any of the HPFRC infill panels after a Design Level Earthquake the effect of an aftershock on the seismic response of a retrofitted steel MRF was simulated with a second Design Level Earthquake and its seismic performance was judged to be better compared to the bare frame.
- Regarding structural damage of the steel moment resisting frame, there was no indication of local buckling to the steel beams in any of the testing phases. The lack of local buckling in part, is attributed to the energy dissipation through micro-cracking in the HPRFC panels during the earthquake. Another reason was due to yielding of the bottom flange of the steel beams in the bare portions between the HPFRC infill panels.
- The numerical models developed to simulate the seismic response of the steel MRF and HPFRC infill panels were validated with the experimental data that became available from the large-scale hybrid simulation tests. These models can be used for further evaluation of a variety of steel buildings retrofitted with HPFRC panels in a performance-based earthquake-engineering context.

9 ACKNOWLEDGEMENTS

This study is based on work supported by the United States National Science Foundation (NSF) under Grant No. CMS-0530383 within the George E. Brown, Jr. Network for Earthquake Engineering Simulation (NEES) Consortium Operations. The Herrick Corporation in Stockton generously donated the steel frame and associated parts of the test setup, including erection. Midstate Precast generously donated the fabrication of the HPFRC infill panels. The financial support of NSF, Herrick and Midstate Precast is gratefully acknowledged. The authors also thank the undergraduate students A. Cantu, D. Ouyang, E. Flores, J. Dory, K. Morales, S. Vanderboll, William Tressler, M.S. (Stanford University), Dr. Andreas Schellenberg, Dr. Selim Gunay, Dr. Shakhzod Tachirov and the rest of the technical staff at the NEES facility at the University of California at Berkeley for their assistance with many aspects of the hybrid simulation testing program. The authors would also like to thank Mr. Ron Hamburger, Mr. David Mar and Dr. Greg Luth for their valuable input regarding the proposed testing phases of the experimental program. Any opinions, findings, and conclusions expressed in this paper are those of the authors and do not necessarily reflect the views of the sponsors.

REFERENCES

[1] ATC-40, The seismic evaluation and retrofit of concrete buildings, ATC-40, Applied Technology Council, Redwood City, CA, 1996.

[2] FEMA 356, Prestandard and commentary for the seismic rehabilitation of buildings, Washington, DC: Federal Emergency Management Agency, 2000.

[3] FEMA 440, Improvement of nonlinear static seismic procedures, Washington, D.C: Federal Emergency Management Agency, 2005.

[4] FEMA 351, Recommended seismic evaluation and upgrade criteria for existing welded steel moment-frame buildings, Washington, DC: Federal Emergency Management Agency, 2000.

[5] FEMA 547, Techniques for the seismic rehabilitation of existing buildings, Washington, DC: Federal Emergency Management Agency, 2006.

[6] S.M. Adan, W. Gibb, Inelastic cyclic testing of the Kaiser bolted bracket moment connection, *Proceedings, Structures Congress*, ASCE, 2008

[7] J.L. Gross, M.D. Engelhardt, C.M. Uang, K. Kasai, N.R. Iwankiw, AISC design guide 12, modification of existing welded steel moment frame connections for seismic resistance, *American Institute of Steel Construction*, Chicago, IL, 1999.

[8] S.A. Civjan, M.D. Engelhardt, J.L. Gross, Slab effects in SMRF retrofit connection tests, *Journal of Structural Engineering*, ASCE, 127 **(3)**: 230-238, 2001.

[9] C.M. Uang, Q.S. Yu, S. Noei, J.L. Gross, Cyclic testing of steel moment connections rehabilitated with RBS or welded haunch, *Journal of Structural Engineering*, ASCE, 126 **(1)**: 157-169, 1999.

[10] C.C. Hung, S. El-Tawil, Seismic behavior of a coupled-wall system with HPFRCC coupling beams, *Proceedings, Structures Congress*, ASCE, 2010.

[11] C.C. Hung, S. El-Tawil, Cyclic model for high performance fiber reinforced cementitious composite structures, *Proceedings, ATC & SEI Conference on Improving the Seismic Performance of Existing Buildings and Other Structures*, ASCE, San Francisco, CA, United States, 2009.

[12] K.E. Kesner, S.L. Billington, Investigation of infill panels made from engineered cementitious composites for seismic strengthening and retrofit, *Journal of Structural Engineering*, ASCE, 131 **(11)**: 1712-1720, 2005.

[13] W.C. Liao, S.H. Chao, S.Y. Park, A.E. Naaman, Self-consolidating high performance fiber reinforced concrete (SCHPFRC) - preliminary investigation, *Report UMCEE 06-02, Dept. of Civil & Environmental Engineering, University of Michigan*, Ann Arbor, MI, 2006.

[14] E.C. Olsen, S.L. Billington, Evaluation of precast, high-performance fiber- reinforced concrete infill panels for seismic retrofit of steel frame building: Phase 1- cyclic testing of single panel components, *Report No. TR 158, John A. Blume Earthquake Engineering Center, Stanford University,* Stanford CA, 2009.

[15] E.C. Olsen, S.L. Billington, Cyclic behavior of precast, self-compacting ductile concrete infill panels for seismic retrofit of steel frame buildings, *ACI Structural Journal*, 108 **(1)**: 51-60, 2011.

[16] J. Hanson, S.L. Billington, Cyclic testing of a ductile fiber-reinforced concrete infill panel system for seismic retrofitting of steel frames, *Report No. TR. 173, John A. Blume Earthquake Engineering Center, Stanford University*, Stanford, CA, 2009.

[17] ASTM, ASTM standard C 1609/C 1609M-05, Standard test method for flexural performance for fiber-reinforced concrete (Using Beam with Third-Point Loading), 2005.

[18] ASCE 41-06, Seismic rehabilitation of existing buildings, ASCE Standard ASCE/SEI 41-06, American Society of Civil Engineers/Structural Engineering Institute, Reston, VA, 2007.

[19] OpenSees, Open System for Earthquake Engineering Simulation, Pacific Earthquake Engineering Research Center (PEER), (http://opensees.berkeley.edu), 2009.

[20] L.F. Ibarra, R.A. Medina, H. Krawinkler, Hysteretic models that incorporate strength and stiffness deterioration. *Journal of Earthquake Engineering and Structural Dynamics*, EESD, 34 **(12)**: 1489–1511, 2005.

[21] D.G. Lignos, H. Krawinkler, Sidesway collapse of deteriorating structural systems under seismic excitations, *Report No. TR 172, John A. Blume Earthquake Engineering Center, Stanford University*, Stanford, CA, 2009.

[22] D.G. Lignos, H. Krawinkler, Deterioration modeling of steel components in support of collapse prediction of steel moment frames under earthquake loading, *Journal of Structural Engineering*, ASCE, (accepted for publication), 2011.

[23] H. Krawinkler, "Shear in Beam-Column Joints in Seismic Design of Frames", *Engineering Journal*, AISC, 15 **(3)**, 1978.

[24] A. Gupta, H. Krawinkler, Seismic demands for performance evaluation of steel moment resisting frame structures, *Report No. TR 132, The John A. Blume Earthquake Engineering Research Center, Department of Civil Engineering, Stanford University*, Stanford, CA, 1999.

[25] P.D. Moncarz, H. Krawinkler, Theory and application of experimental model analysis in earthquake engineering, *Report No. TR 50, John A. Blume Earthquake Engineering Center, Department of Civil Engineering, Stanford University*, Stanford, CA, 1981.

[26] H.G. Harris, G.M. Sabnis, Structural modeling and experimental techniques, 2nd edition, CRC Press, 1999.

[27] M. Nakashima, M. Kato, E. Takaoka, Development of real-time pseudo dynamic testing. *Journal of Earthquake Engineering and Structural Dynamics*, EESD, 21**(1)**: 79-92, 1992.

[28] S.A. Mahin, P.B. Shing, C.R. Thewalt, R.D. Hanson, Pseudodynamic test method - Current status and future direction, *Journal of Structural Engineering*, ASCE, 115**(8)**: 2113-2128, 1989.

[29] A.H. Schellenberg, S. Mahin, G. Fenves, Software framework for hybrid simulation of large structural systems, *Proceedings, Structures Congress*, ASCE, Long Beach, CA, United States, 2007.

[30] A.H. Schellenberg, Advanced implementation of hybrid simulation, *PhD Dissertation*, Civil and Environmental Engineering, University of California Berkeley, Berkeley, CA, 2008.

[31] D.G. Lignos, S.L. Billington, Hybrid testing of a retrofitted steel moment resisting frame with high performance fiber reinforced concrete infill panels, *Proceedings 9th US National and 10th Canadian Conference on Earthquake Engineering: Reaching Beyond Borders*, July 25th-29th, Toronto, Canada, 2010.

[32] S.L. Billington, D.G. Lignos, J.V. Hanson, D.M. Moreno-Luna, Response of high performance fiber reinforced concrete infill panels retrofitting steel moment-resisting frames, *Proceedings, 8th International Conference in Urban Earthquake Engineering, Tokyo Institute of Technology*, March 7-8, Tokyo, Japan, 2011.

[33] W. McGuire, R.H. Gallagher, R.D. Zeimian, Matrix structural analysis, 2nd edition, John Wiley & Sons, Inc, 2000.